

Plasma Protein Profiling for Diagnosis of Pancreatic Cancer Reveals the Presence of Host Response Proteins

John M. Koomen,¹ Lichen Nancy Shih,²
Kevin R. Coombes,³ Donghui Li,⁴ Lian-chun Xiao,³
Isaiah J. Fidler,² James L. Abbruzzese,⁴ and
Ryuji Kobayashi¹

Departments of ¹Molecular Pathology, ²Cancer Biology, ³Biostatistics and Applied Mathematics, and ⁴Gastrointestinal Medical Oncology, University of Texas M.D. Anderson Cancer Center, Houston, Texas

ABSTRACT

Plasma protein profiling using separations coupled to matrix-assisted laser desorption ionization mass spectrometry (MALDI MS) has great potential in translational research; it can be used for biomarker discovery and contribute to disease diagnosis and therapy. Previously reported biomarker searches have been done solely by MS protein profiling followed by bioinformatics analysis of the data. To add to current methods, we tested an alternative strategy for plasma protein profiling using pancreatic cancer as the model. First, offline solid-phase extraction is done with 96-well plates to fractionate and partially purify the proteins. Then, multiple profiling and identification experiments can be conducted on the same protein fractions because only 5% of the fractions are used for MALDI MS profiling. After MALDI MS analysis, the mass spectra are normalized and subjected to a peak detection algorithm. Over three sets of mass spectra acquired using different instrument variables, ~400 unique ion signals were detected. Classification schemes employing as many as eight individual peaks were developed using a training set with 123 members (82 cancer patients) and a blinded validation set with 125 members (57 cancer patients). The sensitivity of the study was 88%, but the specificity was significantly lower, 75%. The reason for the low specificity becomes apparent upon protein identification of the ion signals used for the classification. The identifications reveal only common serum proteins and components of the acute phase response, including serum amyloid A, α -1-antitrypsin, α -1-antichymotrypsin, and inter- α -trypsin inhibitor.

Received 6/28/04; revised 9/16/04; accepted 9/29/04.

Grant support: Goodwin family fund, the Topfer family fund, and M.D. Anderson Cancer Center.

The costs of publication of this article were defrayed in part by the payment of page charges. This article must therefore be hereby marked *advertisement* in accordance with 18 U.S.C. Section 1734 solely to indicate this fact.

Note: J. Koomen and L. Nancy Shih contributed equally to this work.

Requests for reprints: Ryuji Kobayashi, Department of Molecular Pathology, University of Texas M.D. Anderson Cancer Center, 1515 Holcombe Boulevard, Houston, TX 77030. Phone: 713-745-3363; Fax: 713-794-1294; E-mail: rkobayas@mail.mdanderson.org.

©2005 American Association for Cancer Research.

INTRODUCTION

Disease marker discovery is one of the most promising applications of biological mass spectrometry (MS; refs. 1–13). In addition to structural analysis of proteins in biomedical research, MS is now being used to search for biomarkers in extremely complex mixtures (1–13), quantify changes in protein abundance (14), and generate profiles for diagnosis of different disease states by direct analysis of proteins extracted from biological fluids (15, 16), cells (17, 18), and tissues (19, 20). Surface-enhanced laser desorption ionization (SELDI), the coupling of surface retentate chromatography with matrix-assisted laser desorption ionization (MALDI) MS, is already widely used for clinical and translational research, because of the convenient packaging of a low resolution, automated time-of-flight (TOF) mass spectrometer with ready-made “chips” modified with different functional groups for performing surface retentate chromatography (21–23). Despite limitations in sensitivity and difficulties associated with protein identification, profiling still has great value. This technique consists of three steps: separations, mass spectrometry detection, and bioinformatics analysis. In the first step, a population of proteins is extracted from serum or plasma and fractionated because it selectively binds to the SELDI chip. In the second step, the MALDI matrix is added and the proteins are detected using TOF mass spectrometry. In the third, bioinformatics techniques are used to process the mass spectra and generate patterns, which could be used for diagnosis. Because most (~90%) of the ion signals observed in profiling experiments do not correspond to full-length, unmodified proteins, measurement of the intact molecular weights as well as sequence determinations are critical for understanding the structures and functions of these peptides and low molecular weight proteins. Therefore, we have developed analogous methods using 96-well solid-phase extraction discs for offline parallel protein fractionation followed by MALDI MS detection using any mass spectrometry platform (see Fig. 1). Also, fractionated proteins are retained for subsequent structural analysis.

In this paper, we report the initial use of this protocol on a set of pancreatic cancer patients and corresponding controls. The methods for analysis are described in detail. A classification scheme developed by peak-based bioinformatics using several ion signals observed in the mass spectra had 88% sensitivity and 75% specificity. Identification of the ion signals was done for several of the potential biomarkers. The utility and limitations of this method for patient diagnosis are discussed, particularly in light of the proteins that are detected to be different in the MALDI MS profiles.

MATERIALS AND METHODS

Plasma Collection and Processing. Plasma samples came from an ongoing case control study of pancreatic cancer conducted at the University of Texas M.D. Anderson Cancer Center (M.D. Anderson Cancer Center Institutional Review

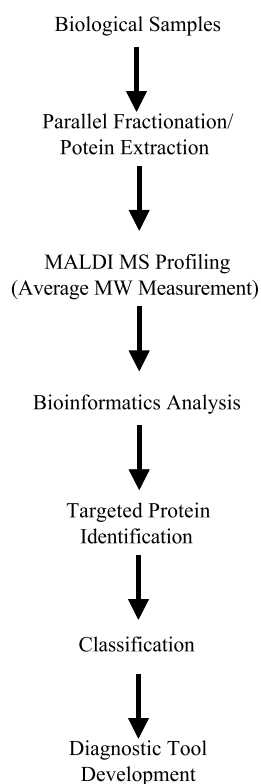


Fig. 1 Experimental flowchart for protein profiling. Proteins are extracted from plasma and fractionated using SPE in 96-well plates. MALDI MS analysis is done on the fractions. After visual inspection and peak-based bioinformatics analysis, ion signals are targeted for identification. Then, the samples are classified as cancer or control. Based on the protein identification and classification results, potential diagnostic tools can be formulated.

Board ID98-155). Cases were patients with a pathologically confirmed ductal adenocarcinoma of the pancreas with no restriction on age, sex, or race. Controls were cancer-free individuals who were accompanying patients with variety types of cancer seen at the Radiology Clinic of M.D. Anderson Cancer Center. Cases and controls were matched by age (± 5 years), sex, and race. An informed consent was obtained from each study participant for an interview and a blood sample. Information on cigarette smoking, alcohol consumption, work history, family history of cancer, and medical history was collected by personal interview using a structured questionnaire. Information on the current disease of the cases (i.e., stage, tumor differentiation, treatment, and survival) was collected from the medical records of the patients. The 274 samples used in the current study were randomly selected from a total of 718 study subjects from the molecular epidemiologic study. Some samples were dropped from the analysis either because of missing clinical data or because we were unable to obtain high quality MALDI spectra. Table 1 contains a summary of the characteristics of the patient samples used in the final analysis.

Blood samples (20 mL) were obtained from patients with pancreatic cancer and control volunteers in heparinized tubes. Plasma was prepared by centrifugation at 2,500 rpm for 10 minutes. Before the preparation of 20 μ L aliquots used for

these experiments, the plasma samples (~ 250 μ L) were centrifuged again at 14,000 rpm for 10 minutes at 4°C to remove particulates and lipids. The 274 samples used in this study were run in four groups (60, 72, 72, and 70) over 4 days because of limits on the number of samples that could be fractionated in parallel (96) and spotted on a MALDI plate (100). The first two groups were chosen for the training set. The second two groups were used for validation. All samples were blinded to the people performing the fractionation and mass analysis.

Protein Extraction and Fractionation. Before protein extraction, all samples were randomized. To increase binding capacity when compared with SELDI or pipette tip-based separations, proteins were extracted from plasma using C1896-well solid-phase extraction discs (Empore, 3M, St. Paul, MN) on a 96-well plate handling robot (Quadra96, Tomtec, Hamden, CT) using the following solvent system for washing: 2% acetonitrile and 0.1% formic acid. Aliquots of plasma (20 μ L) were diluted with 100 μ L of the wash solvent. After loading, the extraction discs were washed with six times with 300 μ L of aqueous 2% acetonitrile with 0.1% formic acid. Two elution steps were done with 300 μ L of aqueous 25% acetonitrile with 0.1% formic acid and then 300 μ L of aqueous 70% acetonitrile with 0.1% formic acid, referred to as the 25% fraction and 70% fraction, respectively. The eluted protein fractions were concentrated back to the original plasma volume.

Matrix-Assisted Laser Desorption Ionization Mass Spectrometry Protein Profiling. The eluted fractions were randomized again before MALDI MS analysis. MALDI MS analysis was done on dried droplet deposits made from mixing 1 μ L of plasma protein extract with 1 μ L of sinapinic acid at 30 mg/mL concentration in a solvent system of 50% methanol and 50% acetonitrile. Spectra were acquired for positive ions in linear mode using a Voyager DE-STR (Applied Biosystems, Framingham, MA) with variables optimized for myoglobin and bovine serum albumin. For the 25% acetonitrile elution, spectra were acquired only with the myoglobin-optimized method; spectra were acquired from the 70% acetonitrile fraction using both methods.

Spectra were externally calibrated using a single matrix deposit containing myoglobin and thioredoxin standards at the center of the MALDI plate. All samples were analyzed using this initial calibration to retain the same number of points (time bins) per spectrum, simplifying bioinformatics processing. Mass spectra were acquired manually, so that the maximum dynamic range could be obtained without ion signal saturation.

Table 1 Distribution of diagnoses in training and validation sets

Stage	Training	Validation	Total
No cancer	41	73	114
Pancreatitis	3	2	5
Stage I	9	3	12
Stage II	4	0	4
Stage III	12	9	21
Stage IVa	28	13	41
Stage IVb	28	31	59
Total	125	131	256

Bioinformatics Analysis. Individual spectra were processed using the simultaneous peak detection and baseline correction (SPDBC) algorithm developed in-house (24). This algorithm produces a separate list of peak locations, heights, widths, and signal-to-noise ratios for each spectrum. For each fraction (BSA70, MYO25, and MYO70), we aligned peaks from distinct spectra using our MatchPeaks algorithm, which first sorts the peaks in order of decreasing signal-to-noise (S/N) ratio. Alignment starts with the first peak [whose mass-to-charge ratio (m/z) is denoted by X] as an “anchor.” If another peak has $m/z = Y$, we define the relative mass error to be $|X - Y|/X$. The algorithm identifies two peaks if the relative mass error is $<0.15\%$ or if the number of clock-ticks separating the peak locations is at most 10; all peaks satisfying this condition are formed into a single “peak class.” Next, the peak with largest S/N that has not yet been assigned to a class is used as a new anchor, and matching continues until all peaks are assigned to a new peak class. The peak lists produced by SPDBC and MatchPeaks are liberal about including potential peaks with very small S/N ratios. To focus on peak classes that are more likely to represent actual proteins, we include an additional filtering step. We only retained a peak class for further analysis if it satisfied at least one of the following conditions:

1. $S/N > 10$ in at least one spectrum.
2. $S/N > 5$ in at least five spectra.
3. $S/N > 3$ in at least 20 spectra.

Heuristically, these numbers indicate that we have more confidence in a peak if it occurs with large S/N or if it occurs in many spectra.

We use two methods to reduce the number of peaks used in the development of a model to predict whether plasma profiles arise from pancreatic cancer patients or healthy controls. First, we perform two-sample t tests on the log-transformed heights of each peak. We compensate for multiple testing by modeling the set of P s as a β -uniform mixture (25). The model is used to control the false discovery rate (26). Second, we combined a genetic algorithm with Mahalanobis distance (27). Mahalanobis distance is a measure of the separation between two groups of samples; it is the main computational idea underlying linear discriminant analysis (28). As a computational tool, a genetic algorithm is a method for conducting directed random searches in order to find an (approximate) optimal solution to some problem (29, 30). In the present case, we ran the genetic algorithm 100 times to identify sets of five peaks that have large Mahalanobis distance between plasma profiles in pancreatic cancer and in healthy controls.

Peaks that were significant based on the t test or that were included in a solution by the genetic algorithm were retained for a final model-building step using an iterative, forward-selection, greedy algorithm. We began with the peak P_1 that had the largest t statistic. Given a set of peaks $\{P_1, P_2, \dots, P_k\}$, we then ordered all peak sets of the form $\{P_1, P_2, \dots, P_k, Q\}$, as Q varies, by the Mahalanobis distance between healthy and cancer samples. If the classification error on the training set was decreased by one of the top 10 peak sets, we added this peak to

the working set and continued. We stopped when the training classification error stabilized.

Protein Identification. Plasma proteins were identified in three different ways. First, one-dimensional SDS-denatured PAGE was done with 4% to 20% Criterion gels (Bio-Rad, Hercules, CA) to separate the proteins. Bands of the appropriate molecular weight were excised, digested with trypsin, and sequenced using liquid chromatography (LC)-MS/MS on an electrospray ion trap instrument (LCQ DecaXP or LTQ, Thermo, San Jose, CA). Proteins from the same C18 fractions were also separated with reverse phase high-performance liquid chromatography using a 0.5-mm ID Vydac C4 column (Hesperia, CA), followed by fraction collection, MALDI analysis to identify the fractions containing target proteins, and then tryptic digestion and LC-MS/MS of the appropriate fractions for protein identification. LC-MS/MS results were searched against the National Center for Biotechnology Information human database using a licensed copy of SONAR (Genomic Solutions, Ann Arbor, MI). Smaller proteins were also identified by direct MALDI MS/MS. Samples were pre-concentrated using C18 Ziptips (Millipore, Billerica, MA) and eluted with 4 mg/mL α -cyano-4-hydroxycinnamic acid prepared in 50% aqueous acetonitrile. Tandem mass spectrometry analysis was done using a 1 kV MS/MS method on a TOF/TOF instrument (Applied Biosystems, Framingham, MA) with collision gas on and off. Several spectra consisting of 22,500 laser shots were acquired and averaged. Peak lists were generated manually and searched against the MSDB using MS-Tag with no enzyme and methionine oxidation selected (<http://prospector.ucsf.edu>).

Quantitative Analysis of Human Serum Amyloid A by ELISA. Serum amyloid A (SAA) levels in human plasma samples were quantified using a human SAA Immunoassay kit (BioSource International, Inc., Camarillo, CA), according to the manufacturer's instructions with minor modifications. Duplicate plasma samples were diluted 1:1,000 with the sample diluent buffer. Working conjugated anti-human SAA ($1\times$, 50 μ L) was added to each assay well that contained monoclonal antibody specific for human SAA, followed by 50 μ L of either standards or samples. The plates were covered and incubated at 37°C for 1 hour. The supernatants were aspirated thoroughly, and the wells were washed thrice with $1\times$ wash buffer. Then, working p -nitrophenyl phosphate substrate solution (100 μ L), prepared just before use, was added and the plate was again covered and incubated at 37°C for 1 hour. Then, stop solution (50 μ L) was added to each well. After incubating at room temperature for 30 minutes, the absorbance at 450 nm was measured for each well on a CERE UV 900C plate reader (BioTek Instruments, Winooski, VT) after zeroing with blank composed of working p -nitrophenyl phosphate substrate solution and stop solution. All samples with concentration of SAA higher than the standards were further diluted and re-assayed at 1:4,000 and 1:10,000 dilutions. The concentration of SAA in each sample well was reported automatically by the instrument software built into the machine and corrected by the dilution factor.

Quantitative Analysis of Human Haptoglobin by Peroxidase Activity Assay. Haptoglobin levels in human plasma samples were quantified using a haptoglobin assay kit (BioSource International) according to the manufacturer's

instructions with minor modifications. Human plasma samples were diluted at least 10-fold with calibrator diluent prior to assay. Equal volumes of hemoglobin and hemoglobin diluent were mixed (reagent 1), as were chromogen and substrate in the ratio of 9:5 (reagent 2). Calibrator standards (0-2 mg/mL) were prepared as instructed. The calibrators and unknown samples (7.5 μ L) were transferred in duplicate to a 96-well microtiter plate. Reagent 1 (100 μ L) was added to each well and mixed, then reagent 2 (140 μ L) was added to each well. After incubation for 5 minutes at room temperature, the absorbance at 660 nm was measured on CERE UV 900C plate reader (BioTek Instruments). All samples with concentrations of haptoglobin higher than the calibrator standards were diluted further and reassayed. The concentration of haptoglobin in each sample well was reported automatically by the instrument software built into the machine and corrected by the dilution factor.

Quantitative Analysis of Human CA19.9. Measurements of the CA19.9 levels in the cancer patients' plasma samples were done in the M.D. Anderson Cancer Center clinical chemistry laboratory.

RESULTS AND DISCUSSION

Almost all of the ion signals observed in the MALDI mass spectra (see Fig. 2) were below m/z 30,000. A larger number of small proteins and peptides is observed in the 25% acetonitrile elution (Fig. 2A), and more large proteins are observed in the 70% fraction (Fig. 2B and C). To determine peak locations in the MALDI profiles, we applied the SPDBC algorithm to all three fractions of all 124 samples in the training set. In the BSA70 spectra, SPDBC detected between 102 and 152 peaks per spectrum, with a median of 129 peaks. In the MYO25 spectra, SPDBC detected between 232 and 287 peaks per spectrum, with a median of 257 peaks. In the MYO70 spectra, SPDBC detected between 231 and 290 peaks per spectrum, with a median of 258 peaks. We then applied the MatchPeaks algorithm to each fraction. We found 306 distinct peaks among the BSA70 spectra, 522 distinct peaks among the MYO25 spectra, and 514 distinct peaks among the MYO70 spectra. We next filtered the peaks based on S/N , as described in MATERIALS AND METHODS. We ended up with 96 peaks in the BSA70 spectra, 185 peaks in the MYO25 spectra, and 155 peaks in the MYO70 spectra, for a total of 436 peaks. The SPDBC and MatchPeaks algorithms both produce lists of peak locations and widths (i.e., intervals that contain the peak). Peaks were quantified in both the training sets and the test sets by taking the maximum value (if SPDBC found a peak in that spectrum) or the median value (if SPDBC did not find a peak) in the interval. These heights were transformed by computing the base-two logarithm for further analyses.

To identify peaks that were differentially expressed in the cancer samples compared with the normal samples, we performed two-sample t tests on the log-transformed heights of each peak, using β -uniform mixture to bound the false discovery rate at 1%. There are 95 peaks that satisfy this criterion (listed in Supplemental Table 1). The peaks are ordered by increasing P ; thus, the most believable differences are at the top of the list. In

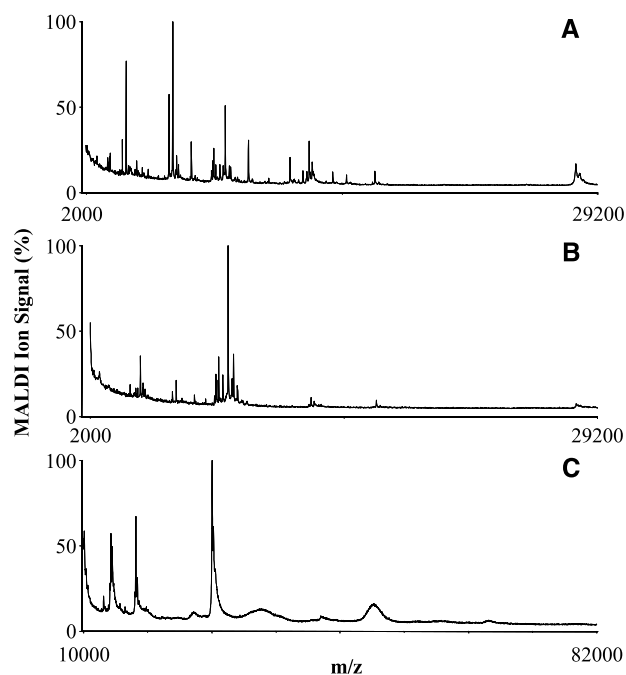


Fig. 2 MALDI MS protein profiles. Proteins were extracted from plasma using reverse phase (C18) solid-phase extraction; representative protein profiles for elution with 25% acetonitrile (A) and 70% acetonitrile (B and C). The spectra in A and B were acquired with instrument variables optimized using apomyoglobin and in C with settings for bovine serum albumin.

the table, positive t statistics correspond to peaks that are overexpressed in cancer, and negative t statistics correspond to peaks that are underexpressed in cancer. The overall most significant peak was found in the BSA70 fraction at m/z 51,534, with a 6.62 t statistic. The most significant peak in the MYO70 fraction was observed at m/z 51,778, with a 5.02 t statistic. Because peaks are fairly broad when the mass is that large, it is possible that both of these peaks represent the same biological substance. The most significant peak in the MYO25 fraction was at m/z 17,240 with a t statistic equal to -5.63 .

To identify sets of peaks that can be used to diagnose pancreatic cancer, we also combined a genetic algorithm with Mahalanobis distance. We used the genetic algorithm to identify sets of five peaks, chosen out of the set of all 436 peaks, that have large Mahalanobis distance between the pancreatic cancer samples and the healthy controls. Because the genetic algorithm uses randomness to locate approximate maxima, it may find different answers each time it is run; therefore, 100 iterations were run from different starting points. As expected, numerous different combinations of five peaks separate normal samples from cancer samples in the training set. Peaks that were significant based on the t test with false discovery rate $<1\%$ or that were included in a solution by the genetic algorithm were used in a greedy algorithm to determine the best predictive model. The algorithm stops adding peaks when the classification error on the training set stops improving.

From the observed ion signals, eight were chosen for patient classification based on the results of the genetic

algorithm and t tests (see Table 2). Zoomed views are shown for six of the eight peaks in Fig. 3; the other two, m/z 19,064 and m/z 39,892, could not be visually distinguished in the MALDI mass spectra. The sensitivity and specificity observed in the validation set for these eight peaks were 95% (54 of 57) and 70% (51 of 73), respectively. After removal of the ion signals that could not be visually observed in the MALDI profiles, the sensitivity and specificity observed in the validation set for these eight peaks were 88% (50 of 57) and 75% (55 of 73), respectively. The sensitivity and specificity for the six peaks with the addition of serum amyloid A were 88% (50 of 57) and 74% (54 of 73). These results are similar to those of other similar studies reported in the literature. The sensitivity is often quite high, but the specificity is poor with 25% to 30% false positives.

To understand the variability in our estimates of the sensitivity and specificity, we used a Bayesian approach to calculate 90% confidence intervals. We assumed that the number of correct classifications (both for cancer and for normal) follows a binomial distribution. We assigned independent β prior distributions $B(\alpha, \beta)$ to the sensitivity and specificity; these prior distributions require us to specify two variables to control the shape and the scale of the β distribution. It is a standard result in

Bayesian statistics that the posterior distribution for the sensitivity or specificity, conditioned on correctly classifying k out of n samples in the validation data, is given by another β distribution, $B(\alpha + k, \beta + n - k)$. The 90% lower and upper limits for sensitivity and specificity of the six-peak model using different prior assumptions are summarized in Table 3. When $\alpha = \beta = 1$, we use a uniform prior, from which the 90% confidence interval for sensitivity ranges from 79.5% to 93.7%, and the 90% confidence interval for specificity ranges from 66.5% to 82.9%. We also considered alternative priors. Using $\alpha = 0.2$ and $\beta = 1.8$ is a skeptical prior, because it suggests that we start the experiment expecting only 10% of the samples to be correctly classified by the model. By contrast, the prior with $\alpha = 1.6$ and $\beta = 0.4$ is fairly aggressive, because it suggests that we start the experiment expecting about 80% of the samples to be correctly classified. In our case, the skeptical estimate yields a lower limit of 87.8% for the sensitivity and a lower limit of 65.4% for the specificity. The more aggressive estimate yields sensitivity between 80.7% and 94.4% and specificity between 67.4% and 83.6%.

Protein identification was attempted for all six peaks used in the classification scheme. The peak at 4,284 was identified as a fragment of inter- α -trypsin inhibitor heavy chain H4 (ITH4)

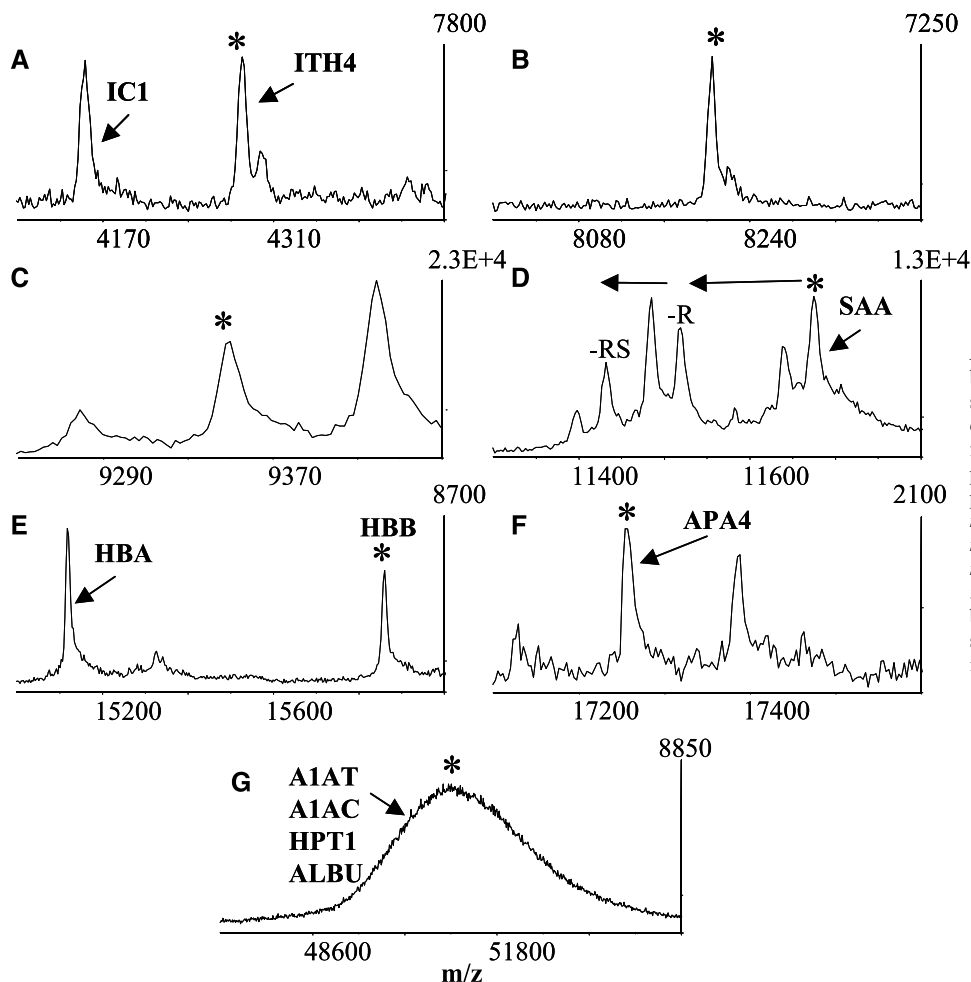


Fig. 3 Ion signals targeted by bioinformatics analysis and visual inspection. Zoomed regions of the mass spectra are shown for several ion signals chosen for protein identification and sample classification: m/z 4,284 (A), m/z 8,204 (B), m/z 9,351 (C), m/z 11,680 (D), m/z 15,863 (E), m/z 17,240 (F), and m/z 51,534 (G). Ion signals are labeled with the SwissProt accession code for the corresponding identified proteins.

Table 2 Ion signals chosen for sample classification and protein identification

No.	<i>m/z</i>	MALDI profile	Mahalanobis distance	<i>T</i> score	False (–)	False (+)	Identification
1	51,534	BSA70	NA	6.62	8	22	α-1-Antitrypsin, α-1-Antichymotrypsin, Haptoglobin
2	17,240	MYO25	2.35	–5.63	8	14	Apolipoprotein A-I or Gln-I
3	15,863	MYO70	2.56	2.04	6	12	Hemoglobin β
4	19,064	MYO70	2.82	–3.78	6	8	Not observed
5	8,204	MYO70	3.08	2.27	6	6	None
6	4,284	MYO25	3.26	–2.43	5	6	Inter-α-trypsin inhibitor
7	39,892	MYO25	3.37	0.96	4	6	Not observed
8	9,351	MYO70	3.66	–3.60	4	5	None

NOTE. The coding for the mass spectra is as follows: MYO25 and MYO70 correspond to the 25% and 70% acetonitrile elutions analyzed the instrument optimized using myoglobin; BSA70 corresponds to the 70% ACN fraction analyzed the instrument optimized using bovine serum albumin.

The Mahalanobis distance and *T* scores are reported for each peak; positive *T* scores indicate an increase in peak intensity in cancer patients' sample when compared to controls. Peaks are listed in the order they were added to the multivariate model by the greedy algorithm.

The number of misclassifications by the cumulative model in the validation set using all peaks selected is listed as false negatives and false positives for each peak. Peaks 4 and 7 were not observed visually during manual inspection of the data: thus, no attempt was made to identify them. Peaks 5 and 8 could not be identified.

by direct MALDI MS/MS (see Fig. 4). The sequence was the only possible match using MS-Tag and searching 14 fragment ions. The prediction of the sequence from ITH4 was consistent in mass accuracy and the cleavages were consistent with expected fragment ion chemistry (i.e., preferential cleavage at aspartic acid and proline). Additional fragment ions were identified manually to verify the proper sequence was selected. The peaks at *m/z* 17,240 and *m/z* 51,534 were identified by one-dimensional SDS-PAGE separation, in-gel digestion, and LC-MS/MS peptide sequencing. The peak at *m/z* 15,863 was identified by C4 high-performance liquid chromatography, fraction collection, MALDI monitoring, in-solution digestion of the appropriate fraction, and LC-MS/MS as hemoglobin β (eight peptides). The peak at 17,240 corresponds to a fragment of apolipoprotein A-I or apolipoprotein glutamine-I (both proteins have the same sequence). Because of the width of the peak at *m/z* 51,534 in the MALDI profiles, it is likely to consist of a combination of proteins. Based on in-gel digestion and LC-MS/MS, α-1-antitrypsin (nine peptides), α-1-antichymotrypsin (four peptides), and haptoglobin (five peptides) could all be detected as components of this broad peak in the MALDI mass spectra (Table 4). In addition to the eight peaks described above, serum amyloid A (*m/z* 11,683) was identified by SDS-PAGE separation, in-gel digestion and LC-MS/MS peptide sequencing (three peptides) as well as C4 high-performance liquid chromatography separation, MALDI detection, and LC-MS/MS peptide sequencing (two peptides), after it was observed primarily in cancer patients (one exception). The entire pattern of peaks in Fig. 3D is consistent with the identification of serum amyloid A. This cluster of peaks was consistently observed in SAA+ patients. Two isoforms of SAA are observed at *m/z* 11,684 and *m/z* 11,629. The lower molecular weight peaks were identified, not by their intact molecular weights, but by the mass differences from the SAA ion signals. The molecular weights could be accurately measured to within 0.5 Da using internal calibration, the mass differences corresponding to arginine residues (156) and serine residues (87) were measured consistently and observed from both intact species. This evidence was very convincing, especially in light of the fact that this pattern of peaks was previously identified as SAA with

tandem mass spectrometry after immunoprecipitation coupled to MALDI MS analysis (33).

Based on the protein identifications, both haptoglobin and serum amyloid A levels were measured in different aliquots of the same set of samples used for protein profiling to determine whether either has diagnostic value for pancreatic cancer patients. A two-sample *t* test of measurements of serum haptoglobin showed no evidence of differential expression between cancer patients and healthy individuals ($t = 1.0265$, $P = 0.31$). However, serum amyloid A was significantly differentially expressed ($t = 3.82$, $P = 0.0002$). Of the 113 healthy individuals, 112 had SAA levels below 100; the last individual was an extreme outlier with an SAA level of 445.2. Using SAA > 100 as our criterion, we are able to improve

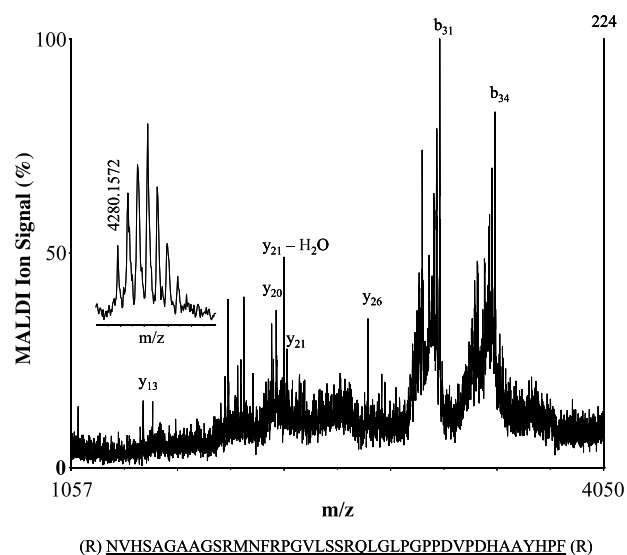


Fig. 4 Inter-α-trypsin inhibitor H4 is identified by MALDI MS/MS of *m/z* 4,284. The inset shows the high-resolution mass spectrum for the parent ion before mass selection. The cleavages indicated occur preferentially at either proline or aspartic acid residues, which is consistent with the expected fragmentation pattern. Bottom, sequence along with the neighboring residues.

Table 3 The 90% lower and upper limits for sensitivity and specificity of the six-peak model

α	β	Lower	Upper
Sensitivity			
0.2	1.8	0.778	0.926
1	1	0.795	0.937
1.6	0.4	0.807	0.944
Specificity			
0.2	1.8	0.654	0.820
1	1	0.665	0.829
1.6	0.4	0.674	0.836

sensitivity for pancreatic cancer by adding an SAA screen compared with using CA19.9 alone. Of the 23 cancer patients that present with low CA19.9 levels, seven (2 stage III, 2 stage IVa, and 3 stage IVb) have high levels of SAA.

Furthermore, using the ELISA results for serum amyloid A, a detection limit can be assessed for this MALDI profiling. We could detect SAA in almost all samples above 50 $\mu\text{g}/\text{mL}$, which corresponds to 4.28 $\text{pmol}/\mu\text{L}$ and a 4.28 $\mu\text{mol}/\text{L}$ solution of the SAA protein. The highest SAA concentration that the MALDI could not detect was 61.6 $\mu\text{g}/\text{mL}$ (5.3 $\mu\text{mol}/\text{L}$) and the lowest it could detect was 20.9 $\mu\text{g}/\text{mL}$ (1.8 $\mu\text{mol}/\text{L}$). These results compare favorably to the practical limits of instrument performance (protein detection at 100 fmol to 1 pmol), considering the source of the protein, its presence in an extremely complex mixture, and the fact that it is processed in plasma and thus seems as multiple peaks in the MALDI mass spectra (see Fig. 3D). This result is very important because it links the MALDI data to concentration measurements and is consistent with the claim that protein profiling using simple fractionation coupled to direct MALDI MS analysis will not be able to detect proteins which are low in abundance (31, 32).

CONCLUSIONS

The TOF MS instrument performance in both mass resolution and mass measurement accuracy and the capacity and reproducibility of the 96-well plate solid-phase extraction fractionation are better than in SELDI experiments. For ion signals between m/z 2,000 and m/z 30,000, the resolving power for this linear TOF mass spectrometer ranges from 500 to 1,000 in these experiments, compared with 100 to 400 for SELDI instruments. Even with a single external calibration at the center of the plate, the deviation in mass measurement of apolipoprotein C1 at m/z 6,631 was less than +3 and the deviation in mass measurement of hemoglobin α at m/z 15,127 was less than +6

across the entire sample set; both of these values are below a mass measurement error of 0.05%. With internal calibration, mass measurement error could be decreased to <0.01% (100 ppm) for these peptides and low molecular weight proteins. Furthermore, we have established the detection limits of this technique to be at the level of a 5 $\mu\text{mol}/\text{L}$ protein concentration by comparison of the MALDI mass spectra and ELISA measurements of serum amyloid A. This value compares favorably to the practical limits for detection of an individual protein in a protein mixture with MALDI TOFMS (hundreds of femtomoles to a few picomoles), because of the observation of SAA as several peaks due to NH_2 -terminal modification (33) and the complexity and contamination of the protein's source, plasma. In addition to improving the characteristics of the protein profiling experiment, the utility of sequencing by direct MALDI MS/MS was shown in the identification of the ion signal at m/z 4,284 observed at higher intensity in controls as a fragment of inter- α -trypsin inhibitor H4. A similar peak was observed in a SELDI study of pancreatic cancer (m/z 4,277), but the identity was not reported in that study (34). Direct MALDI MS/MS is a useful tool for obtaining sequence information and establishing validity for the ion signals observed in these protein profiles.

Despite significant improvements in the protein fractionation and mass spectrometry, the classification results are similar to those of other plasma or serum protein profiling studies reported in the literature. The sensitivity is often quite high (>90%), but the specificity is not sufficient (70–75%). A test with these characteristics gives too many false positives, perhaps leading clinicians to give unnecessary treatment. The low specificity is consistent with the protein identifications: the proteins do not have specific roles in pancreatic cancer, but rather in host response. SAA and haptoglobin are constituents of the acute phase response. Despite prior reports which link these proteins to cancer (35–43), we believe that these proteins will not be specific enough for cancer diagnosis, because they are also observed in other diseases involving inflammation, including coronary disease and bacterial infection (44–48). Indeed, measurements of plasma haptoglobin were not useful for diagnosis of pancreatic cancer in the population studied here. Based on the increased levels of SAA in a subset of cancer patients (~30%), 7 of 137 (~5%) pancreatic cancer patients were diagnosed that could have been missed by CA19.9 measurements; therefore, SAA may have some value as a supplement to conventional tests. Unlike SAA and haptoglobin, increased expression of plasma protease inhibitors is consistent

Table 4 Peptide sequences and the target proteins identified by LC-MS/MS

Protein	Profile m/z	Peptide sequences
Serum amyloid A	11,684	SFFSFLGEAFD GAR LTGHGAEDSLADQAANK FFGHGAEDSLADQAANEWGR
Hemoglobin β	15,863	VHLTPEEK SAVTALWGK VNVDEVGGEALGR LLVVYPWTQR VVAGVANALAHK EFTPPVQAAAYQK KFTPPVQAAAYQK FFESFGDLSTPDVAVMGNPK KVLGAFSDGLAHLNLIK
Apolipoprotein A-I (Gln I)	17,240	QGLLPVLESFK THLAPYSDEL R DYVSQFQSALGK VKDLATVYVDV LK DSGRDYVSQFQGSALGK
α -1-Antitrypsin	51,534	WERPFVVK LSITGTYDLK LVDFKLEDFVKK LQHLENLTHDIITK VFSNGADLSGVTEEAPLK LYHSEAFVTFNGDTEEAK(K) TLNQPDSQLQLTTGNGLFLSEGLK GTEAAGAMFLEAIPMSIPPEVK WERPFVVKDTEEEDFHVDQVTTVK
α -1-Antichymotrypsin	51,534	EIGELYLPK LYGSEAFATDFQDSAAAK AVLDVFEEGTEASAATAVK HPNSPLDEENLTQENQDR
Haptoglobin	51,534	GSPFWQAK DIAPTLTLYVGK VTSIQDWVQK TEGDGVYTLNDK(K) LRTEGDGVYTLNNEK

with and seems more specific for pancreatic cancer. Furthermore, the serpins, α -1-antitrypsin and α -1-antichymotrypsin, have been directly linked to pancreatic cancer (49–54). However, the important caveat is that these proteins also play a role in the acute phase response, so we can not conclusively state that a specific diagnostic marker is being observed. Based on these protein identities and the previous literature (49–54), it is unlikely that these markers are specific for diagnosis of pancreatic cancer. The unidentified peaks (m/z 8,204 and m/z 9,351) are too high in m/z for direct MALDI MS/MS and they have proven to be difficult to isolate chromatographically.

Although improvements were made to the fractionation and mass analysis and differences could be detected between cancer patients and corresponding controls, critical limitations still exist for this technology. The sensitivity of MALDI protein profiling remains poor when compared with antibody-based methods, as previously pointed out by Diamandis (31, 32). Furthermore, protein profiling experiments are restricted to the limited mass range for protein detection with MALDI TOF MS (most ion signals between m/z 2,000 and m/z 30,000). In the future, we will pursue other analytic methods, including profiling enzymatic digests of plasma proteins, which not only increase the sensitivity and widen the accessible mass range for the protein detection, but also enable direct identification using tandem mass spectrometry peptide sequencing.

ACKNOWLEDGMENTS

We thank Andrea Cervin and Rebecca Liu for assistance with protein fractionation and Dr. Stanley Hamilton for his valuable comments throughout the course of these experiments.

REFERENCES

- Petricoin EF, Ardekani AM, Hitt BA, et al. Use of proteomic patterns in serum to identify ovarian cancer. *Lancet* 2002;359:572–7.
- Steel LF, ShumPERT D, Trotter M, et al. A strategy for the comparative analysis of serum proteomes for the discovery of biomarkers for hepatocellular carcinoma. *Proteomics* 2003;3:601–9.
- Rai AJ, Zhang Z, Rosenzweig J, et al. Proteomic approaches to tumor marker discovery. *Arch Pathol Lab Med* 2002;126:1518–26.
- Li J, Zhang Z, Rosenzweig J, Wang YY, Chan DW. Proteomics and bioinformatics approaches for identification of serum biomarkers to detect breast cancer. *Clin Chem* 2002;48:1296–304.
- Adam B-L, Qu Y, Davis JW, et al. Serum protein fingerprinting coupled with a pattern-matching algorithm distinguishes prostate cancer from benign prostate hyperplasia and healthy men. *Cancer Res* 2002;62:3609–14.
- Srinivas PR, Srivastava S, Hanash S, Wright GL Jr. Proteomics in early detection of cancer. *Clin Chem* 2001;47:1901–11.
- Seliger B, Kellner R. Design of proteome-based studies in combination with serology for the identification of biomarkers and novel targets. *Proteomics* 2002;2:1641–51.
- Bergquist J, Palmblad M, Wetterhall M, Hakansson P, Markides KE. Peptide mapping of proteins in human body fluids using electrospray ionization Fourier transform ion cyclotron resonance mass spectrometry. *Mass Spectrom Rev* 2002;21:2–15.
- Rosty C, Christa L, Kuzdzal S, et al. Identification of hepatocarcinoma-intestine-pancreas/pancreatitis-associated protein I as a biomarker for pancreatic ductal adenocarcinoma by protein biochip technology. *Cancer Res* 2002;62:1868–75.
- Heine G, Zucht H-D, Schuhmann MU, et al. High-resolution peptide mapping of cerebrospinal fluid: a novel concept for diagnosis and research in central nervous system diseases. *J Chromatogr B* 2002;782:353–61.
- Desiderio D. Mass spectrometric analysis of neuropeptidergic systems in the human pituitary and cerebrospinal fluid. *J Chromatogr B* 1999;731:3–22.
- Vlahou A, Schellhammer PF, Mendrinis S, et al. Development of a novel proteomic approach for the detection of transitional cell carcinoma of the bladder in urine. *Am J Pathol* 2001;158:1491–502.
- Spahr CS, Davis MT, McGinley MD, et al. Towards defining the urinary proteome using liquid chromatography-tandem mass spectrometry. I. Profiling an unfractionated tryptic digest. *Proteomics* 2001;1:93–107.
- Gygi SP, Rist B, Gerber SA, Turecek F, Gelb MH, Aebersold R. Quantitative analysis of complex protein mixtures using isotope-coded affinity tags. *Nat Biotechnol* 1999;17:994–9.
- Sinz A, Bantscheff M, Mikkat S, et al. Mass spectrometric proteome analyses of synovial fluids and plasmas from patients suffering from rheumatoid arthritis and comparison to reactive arthritis or osteoarthritis. *Electrophoresis* 2002;23:3445–56.
- Catinella S, Seraglia R, Marsilio R. Evaluation of protein profile of human milk by matrix-assisted laser desorption/ionization mass spectrometry. *Rapid Commun Mass Spectrom* 1999;13:1546–9.
- Palmer-Toy DE, Sarracino DA, Sgroi D, LeVangie R, Leopold PE. Direct acquisition of matrix-assisted laser desorption/ionization time-of-flight mass spectra from laser capture microdissected tissues. *Clin Chem* 2000;46:1513–6.
- Xu BJ, Caprioli RM, Sanders ME, Jensen RA. Direct analysis of laser capture microdissected cells by MALDI mass spectrometry. *J Am Soc Mass Spectrom* 2002;13:1292–7.
- Caprioli RM, Farmer TB, Gile J. Molecular imaging of biological samples: localization of peptides and proteins using MALDI-TOF MS. *Anal Chem* 1997;69:4751–60.
- Stoeckli M, Farmer TB, Caprioli RM. Automated mass spectrometry imaging with a matrix-assisted laser desorption ionization time-of-flight instrument. *J Am Soc Mass Spectrom* 1999;10:67–71.
- Hutchens TW, Yip TT. New desorption strategies for the mass spectrometric analysis of macromolecules. *Rapid Commun Mass Spectrom* 1993;7:576–80.
- Weinberger SR, Boschetti E, Santambien P, Brenac V. Surface-enhanced laser desorption-ionization retentate chromatography mass spectrometry (SELDI-RC-MS): a new method for rapid development of process chromatography conditions. *J Chromatogr B Analyt Technol Biomed Life Sci* 2002;782:307–16.
- Issaq HJ, Conrads TP, Prieto DA, Tirumalai R, Veenstra TD. SELDI-TOF MS for diagnostic proteomics. *Anal Chem* 2003;75:148–55A.
- Coombes KR, Fritsche HA Jr, Clarke C, et al. Quality control and peak finding for proteomics data collected from nipple aspirate fluid using surface enhanced laser desorption and ionization. *Clin Chem* 2003;49:1615–23.
- Pounds S, Morris SW. Estimating the occurrence of false positives and false negatives in microarray studies by approximating and partitioning the empirical distribution of p-values. *Bioinformatics* 2003;19:1236–42.
- Benjamini Y, Hochberg Y. Controlling the false discovery rate: a practical and powerful approach to multiple testing. *Journal of the Royal Statistical Society, Series B* 1995;57:289–300.
- Baggerly KA, Morris JS, Wang J, Gold D, Xiao LC, Coombes KR. A comprehensive approach to the analysis of MALDI-TOF proteomics spectra from serum samples. *Proteomics* 2003;3:1667–7.
- Mardia KV, Kent JT, Bibby JM. *Multivariate analysis*. New York: Academic Press; 1979.
- Holland J. *Adaptation in natural and artificial systems*, 3rd ed. Cambridge (MA): MIT Press; 1994.
- Goldberg DE. *Genetic algorithms in search, optimization, and machine learning*. Reading (MA): Addison-Wesley; 1989.
- Diamandis EP. Analysis of serum proteomic patterns for early cancer diagnosis: drawing attention to potential problems. *J Natl Cancer Inst* 2004;96:353–6.

32. Diamandis EP. Mass spectrometry as a diagnostic and a cancer biomarker discovery tool: opportunities and potential limitations. *Mol Cell Proteomics* 2004;3:367–78.
33. Kiernan UA, Tubbs KA, Nedelkov D, Niederkofler EE, Nelson RW. Detection of novel truncated forms of human serum amyloid A protein in human plasma. *FEBS Lett* 2003;537:166–70.
34. Koopmann J, Zhang Z, White N, et al. Serum diagnosis of pancreatic adenocarcinoma using surface-enhanced laser desorption and ionization mass spectrometry. *Clin Cancer Res* 2004;10:860–8.
35. Cho WC, Yip TT, Yip C, et al. Identification of serum amyloid A protein as a potentially useful biomarker to monitor relapse of nasopharyngeal cancer by serum proteomic profiling. *Clin Cancer Res* 2004;10:43–52.
36. Howard BA, Wang MZ, Campa MJ, Corro C, Fitzgerald MC, Patz EF Jr. Identification and validation of a potential lung cancer serum biomarker detected by matrix-assisted laser desorption/ionization-time-of-flight spectra analysis. *Proteomics* 2003;3:1720–4.
37. O'Hanlon DM, Lynch J, Cormican M, Given HF. The acute phase response in breast carcinoma. *Anticancer Res* 2002;22:1289–93.
38. Kimura M, Tomita Y, Imai T, et al. Significance of serum amyloid A on the prognosis in patients with renal cell carcinoma. *Cancer* 2001;92:2072–5.
39. Glojnaric I, Casl MT, Simic D, Lukac J. Serum amyloid A protein (SAA) in colorectal carcinoma. *Clin Chem Lab Med* 2001;39:129–33.
40. Biran H, Friedman N, Neumann L, Pras M, Shainkin-Kestenbaum R. Serum amyloid A (SAA) variations in patients with cancer: correlation with disease activity, stage, primary site, and prognosis. *J Clin Pathol* 1986;39:794–7.
41. Raynes JG, Cooper EH. Comparison of serum amyloid A protein and C-reactive protein concentrations in cancer and non-malignant disease. *J Clin Pathol* 1983;36:798–803.
42. Rosenthal CJ, Sullivan LM. Serum amyloid A to monitor cancer dissemination. *Ann Intern Med* 1979;91:383–90.
43. Ye B, Cramer DW, Skates SJ, et al. Haptoglobin- α subunit as potential serum biomarker in ovarian cancer: identification and characterization using proteomic profiling and mass spectrometry. *Clin Cancer Res* 2003;9:2904–11.
44. Whicher J, Biasucci L, Rifai N. Inflammation, the acute phase response and atherosclerosis. *Clin Chem Lab Med* 1999;37:495–503.
45. Lowe GD. The relationship between infection, inflammation, and cardiovascular disease: an overview. *Ann Periodontol* 2001;6:1–8.
46. Romette J, di Costanzo-Dufetel J, Charrel M. Inflammatory syndrome and changes in plasma proteins. *Pathol Biol (Paris)* 1986;34:1006–12.
47. Jayle MF, Engler R. Different spectra of blood protein changes in inflammatory conditions. *Pathol Biol (Paris)* 1974;22:645–50.
48. Haag AM, Chaiban J, Johnston KH, Cole RB. Monitoring of immune response by blood serum profiling using matrix-assisted laser desorption/ionization time-of-flight mass spectrometry. *J Mass Spectrom* 2001;36:15–20.
49. Irigoyen Oyarzabal AM, Amiguet Garcia JA, Lopez Vivanco G, et al. Tumoral markers and acute-phase reactants in the diagnosis of pancreatic cancer. *Gastroenterol Hepatol* 2003;26:624–9.
50. Trachte AL, Suthers SE, Lerner MR, et al. Increased expression of α -1-antitrypsin, glutathione *S*-transferase pi and vascular endothelial growth factor in human pancreatic adenocarcinoma. *Am J Surg* 2002;184:642–8.
51. Ito T, Kimura T, Nawata H. Serum elastase 1 appears specific for cancer of the pancreatic head. *Am J Gastroenterol* 1991;86:1778–83.
52. Buamah PK, Skillen AW. Concentrations of protease and anti-protease in serum of patients with pancreatic cancer. *Clin Chem* 1985;31:876–7.
53. Trichopoulos D, Tzonou A, Kalapothaki V, Sparos L, Kremastinou T, Skoutari M. α 1-Antitrypsin and survival in pancreatic cancer. *Int J Cancer* 1990;45:685–6.
54. Lankisch PG, Koop H, Winckler K, Kaboth U. α 1-Antitrypsin in pancreatic diseases. *Digestion* 1978;18:138–40.